

PAPER • OPEN ACCESS

Effect of samarium on microstructure and intermetallic formation in Al-5Zn-0.5Si alloy

To cite this article: D Ferdian *et al* 2019 *IOP Conf. Ser.: Mater. Sci. Eng.* **541** 012024

View the [article online](#) for updates and enhancements.

Effect of samarium on microstructure and intermetallic formation in Al-5Zn-0.5Si alloy

D Ferdian^{1*}, J R Pratama¹, Y Pratesa¹

¹Department of Metallurgy and Materials Engineering, Universitas Indonesia, Depok 16424, Indonesia

Email: deni@metal.ui.ac.id

Abstract. Aluminium-Zinc-Silicon alloy is a material candidate for low voltage sacrificial anode. Nevertheless, iron-rich intermetallic phase that formed in the interdendritic region can reduce its efficiency due to the self-corrosion phenomenon. Samarium addition is expected to modify the formation of iron-rich intermetallic phase. The alloying process was conducted with melting of aluminium and other additional element in mini electric resistance furnace. Furthermore, characterization of the alloys was performed using optical emission spectrometer, differential scanning calorimetry, optical metallography and scanning electron microscopy equipped with energy dispersive spectrometer. The result showed that samarium can refined the secondary dendrite arm spacing (SDAS) from 89.6 μm to 61.4 μm . Samarium also shifted the solidification temperature of the alloy which affected the size of SDAS and formation of $\text{Al}_2\text{Si}_2\text{Sm}$ intermetallic phase.

1. Introduction

The most common type of corrosion protection in offshore structural applications is by cathodic protection method, such as sacrificial anode, impressed current, or coating. Sacrificial anodes method commonly used is attributed to their easy to apply and can be installed without any requirement of external energy. Aluminium Sacrificial Anodes are widely used because they have a good efficiency in the offshore environment. Aluminium Sacrificial Anode has an efficiency up to 25.000 Ah / Kg and driving voltage of -1.1 V vs. SCE.

The first generation alloy used for aluminium sacrificial anode is Al-5Zn-Hg. However, this alloy has been replaced because it is considered not environmentally friendly due to the release of mercury ions during the protection. Current generation of sacrificial anode that widely used is Al-Zn-In alloy. Sakano et al. revealed that indium-activated aluminium alloy anodes with composition is Al- 5Zn-0.03In increase anode efficiency [1]. Furthermore, J.U Chavarin showed that chloride is also important in Al-Zn-In activation [2]. Indium ions made highly polarizing phenomena that promote chloride migration and adsorption, so it increases aluminium dissolution by forming complex chlorides. In general, Al-Zn-In alloy has a good efficiency, nevertheless one of weaknesses is the low potential protection value that could reach -1.1V vs. SCE. As a result, it could causing a stress corrosion cracking (SCC) phenomena on the protected material [3].

New generation of a sacrificial aluminium anode that being develop is low driving voltage anode. This type of sacrificial anode is considered safer to use for steel materials that have high mechanical strength. Ma Li et al. found working potential of Al-Ga alloy was -802 mV ~ -818 mV (vs. Ag / AgCl seawater) respectively [4]. Furthermore, Pratesa et al. [5] is used copper and silicon to substitute gallium



for low voltage properties. It showed that copper and silicon increased potential protection of Al-Zn alloy. However, the presence of iron element triggers the formation of iron-rich intermetallic phase within the product. Thus, this intermetallic phase could initiate more selective corrosion which gives a detrimental effect for effectivity [5].

Samarium (Sm) additions have shown the ability to act as a grain refinement in solidification process [6,7]. With the addition of Samarium element, there is an alteration morphology of α -Al precipitates from dendritic into equiaxed forms [8]. The addition of Sm elements is also expected to improve the shape of the eutectic Si precipitates. Therefore, the objective of this present work is to characterize the effect of Sm on microstructure of Al-5Zn-0.5Si alloy as candidate for low voltage sacrificial anode.

2. Experimental Method

The alloying process was conducted using a mini electric resistance furnace. The alloying material consist of high purity Al ingot (99.5% from Inalum), Al-Si alloy (made from Al ingot and 443 Si grade), Zinc (99% purity) which were used to synthesize Al-Zn-Si alloys under normal ambient atmosphere at 850°C. Samarium element was added using a high purity binary Al-Sm alloy to achieve the desired content of 0.3, 0.6 and 1 wt. % Sm. The result of the process is characterized by differential scanning calorimetry (DSC) with a cooling rate of 10°C·min⁻¹. Moreover, optical emission spectrometer (OES) was used to analyse the chemical composition of the alloy while energy dispersive spectrometer (EDS) was used to investigate the micro chemical composition of the formed phase. Microstructure examination by optical microscope is conducted using metallographic techniques to observe the intermetallic phase and other feature in the matrix.

3. Results And Discussion

The chemical composition test result showed in Table 1. Unfortunately, Sm addition could not be measured due to limitation with the apparatus that was used. Therefore, the addition of Sm is given based on the weight amount of Al-Sm added to the melt. The chemical composition showed no significant decrease in zinc and silicon levels that indicating fading process due to melting processes.

Table 1. Composition of the primary element in Al-5Zn-0.5Si-xSm

	Al	Zn	Si	Fe	Cu	In
Al-5Zn-0.5 Si	94.8	4.55	0.561	0.0345	<0.001	<0.01
Al-5Zn-0.5Si-0.1Sm	94.5	4.74	0.542	0.0690	0.0354	< 0.01
Al-5Zn-0.5Si-0.3Sm	94.7	4.55	0.521	0.0653	<0.001	<0.01
Al-5Zn-0.5Si-0.5Sm	94.8	4.32	0.491	0.0726	0.0029	<0.01

DSC thermograms upon cooling as illustrated in Figure 1 showed the solidification reaction at decreasing temperature of nucleation and growth of primary (Al) dendrites and the existence of second phase (samarium-rich intermetallic phase) formation. It seems that, the precipitation of iron-rich intermetallic phase (β -Al₉Fe₂Si₂) is over shadowed by the peak of primary α -(Al). Formation of Al₂Si₂Sm phase successfully prevented the formation of iron- rich intermetallic phase (β -Al₉Fe₂Si₂ phase). This change is visible at 0.3 Sm addition while at 0.1 Sm is not seen clearly. DSC thermograms also observed a shifting of thermal arrests correspond to the second phase to a higher temperature as the Sm addition increases.

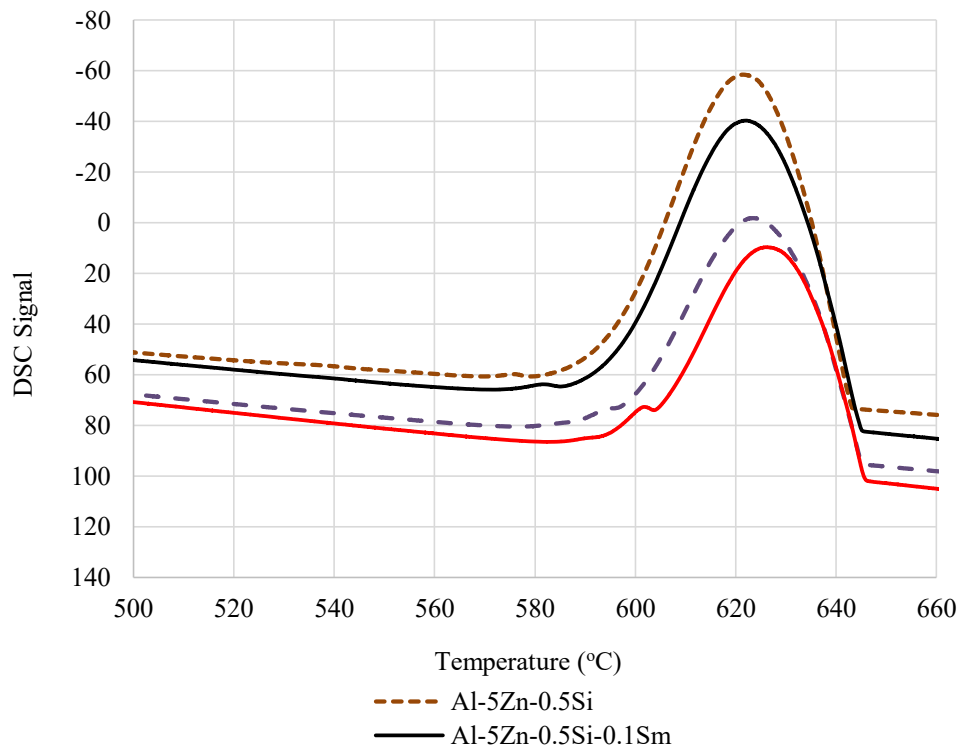


Figure 1. DSC thermograms upon cooling at $10^{\circ}\text{C}\cdot\text{min}^{-1}$ for various samarium additions.

Microstructure of the as-cast samples observed by optical microscopy showed the presence of the (Al) matrix, β -Zn and intermetallic phases in the interdendritic region as seen in figure 2. The presence of undissolved β -Zn within the aluminum matrix causing the damage of passive layer of anode surface [9]. The zinc addition to the alloys also shift the anode potential to more negative value, therefore increases the anode efficiency [10]. Moreover, the result showed a reduction of the SDAS due to Sm addition. This result proved that samarium acted as a grain refinement in aluminium. Measurement showed that the SDAS was successfully reduced from $89.6\ \mu\text{m}$ to $61.4\ \mu\text{m}$ when the alloy was added with 0.5Sm as seen in figure 3. Moreover, the optimum reduction of SDAS was achieved at 0.3Sm additions. Further increase of samarium addition did not give sufficient effect as with 0.3 Sm. At 0.5Sm addition, the ability of samarium to reduce the SDAS is 5% lower compared with 0.3Sm addition. This showed that samarium is no longer acted only as grain refinement but probably served as an intermetallic modifier. This result is confirmed with the DSC result when the new peak occurs at temperature 600°C which belongs to samarium-rich intermetallic phase ($\text{Al}_2\text{Si}_2\text{Sm}$) formation [11,12].

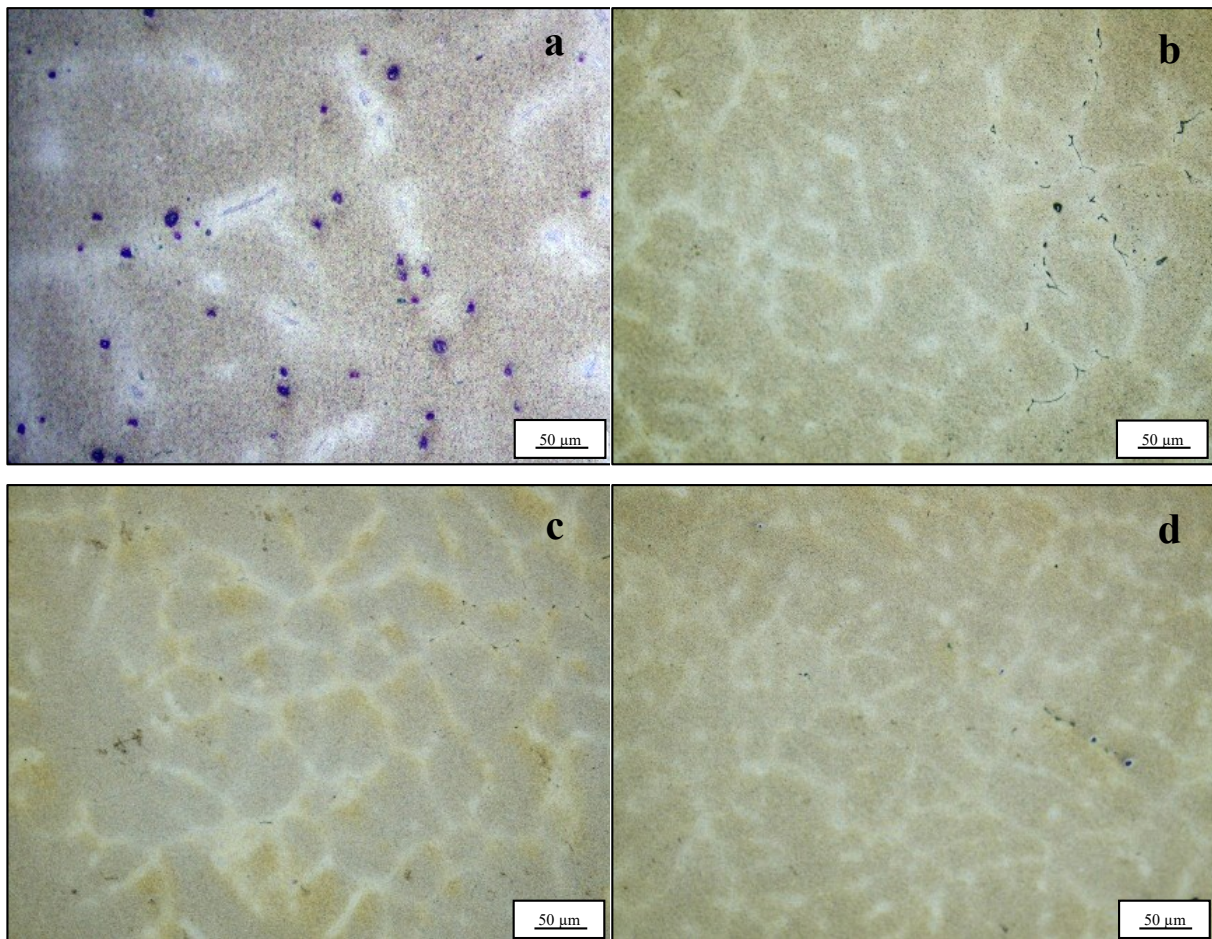


Figure 2. Optical micrograph of as cast Al-5Zn-0.5Si-Sm samples with various samarium additions: (a) 0%, (b) 0.1%, (c) 0.3%, and (d) 0.5%.

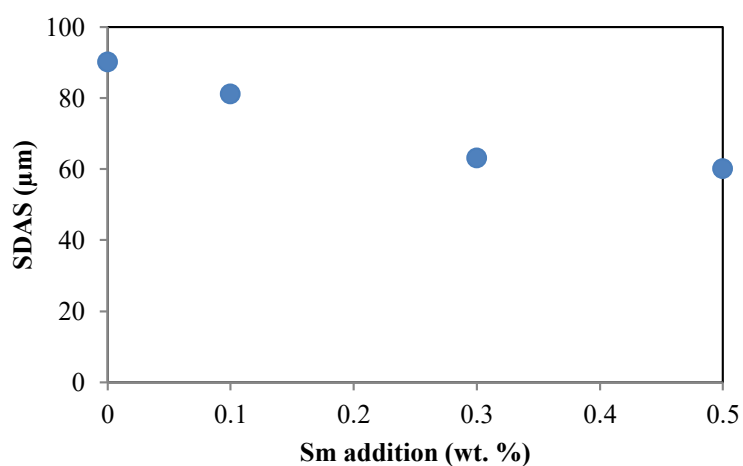


Figure 3. Effect of samarium in SDAS size.

EDS mapping and micro chemical analysis indicate the formation of an intermetallic compound containing samarium. Element mapping as seen in figure 4 showed dispersion of Zn element in the Al matrix while samarium is showed in the interdendritic region along with silicon and other minor element.

Further examination with EDS was conducted at selected area (white circle in figure 4a). The composition of samarium intermetallic compound (spectrum 1) as seen in figure 5 could relate to $\text{Al}_2\text{Si}_2\text{Sm}$ phase [12].

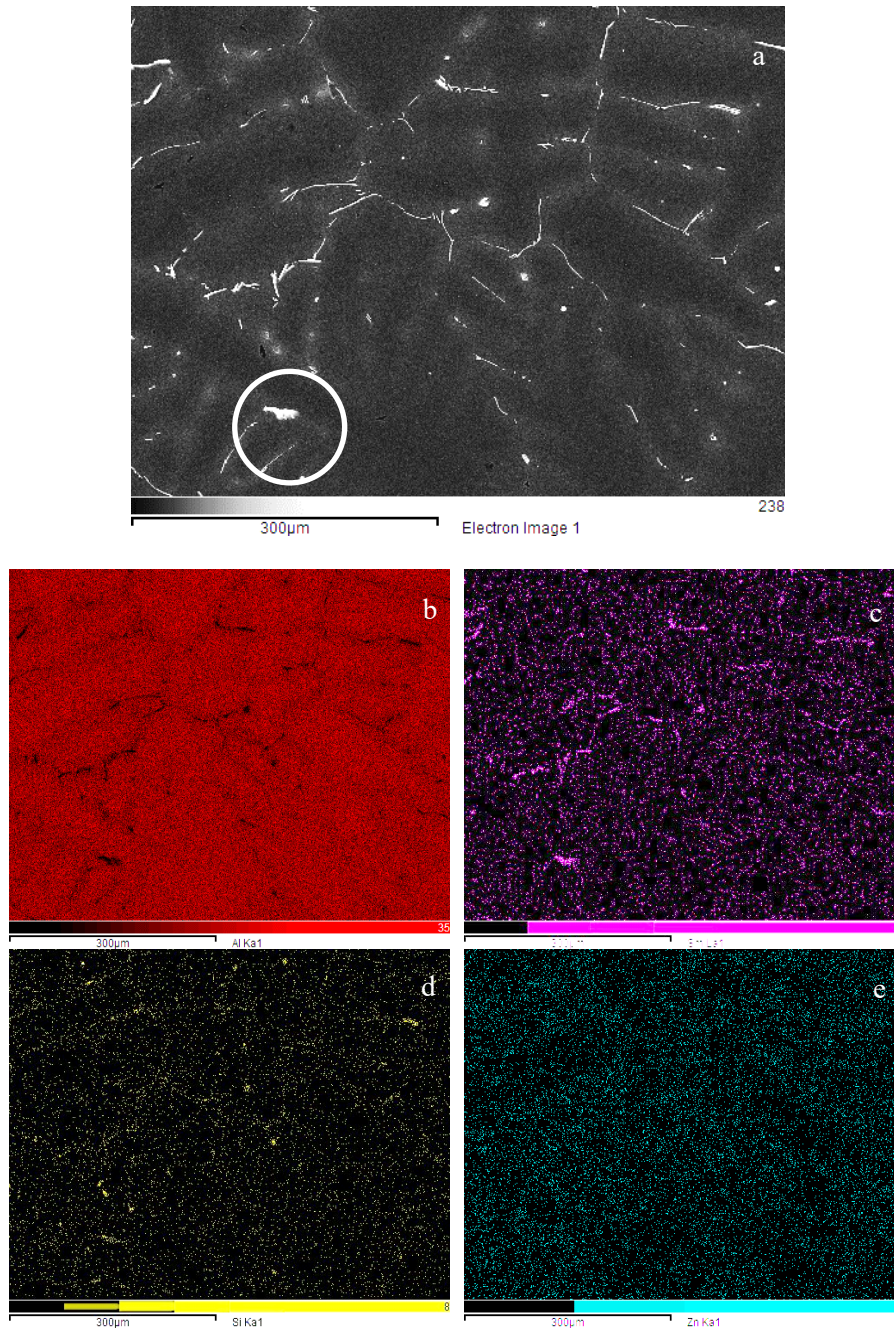
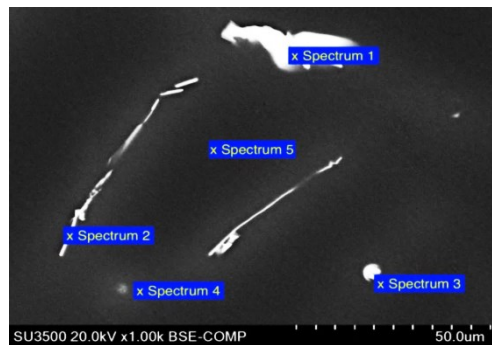


Figure 4. Backscattered electrons SEM micrograph of Al-5Zn-0.5Si-0.5Sm alloy (a) and related EDS mappings of aluminium (b), silicon (c), samarium (d) and zinc (e).



	Composition (at. %)					Phase identification
	Al	Sm	Si	Zn	O	
Spectrum 1	58.76	13.35	12.68	3.09	12.12	Al ₂ Si ₂ Sm
Spectrum 2	76.83	1.04	10.62	2.45	3.45	
Spectrum 3	62.34	3.46	12.99	3.36	6.24	

Figure 5. EDS micro-analysis of the phases in Al-5Zn-0.5Si-0.5Sm alloy taken from BSE image.

4. Conclusion

Sm addition to Al-5Zn-0.5Si form an Al₂Si₂Sm intermetallic precipitate that shift the solidification process as Sm addition increases. Sm addition also reduced SDAS from 89.6 μm to 61.4 μm in 0.5 Sm with 0.3 Sm additions as the optimum reduction.

References

- [1] Sakano M H T and Toda K 1966 *Mater. Prot.* **5** 45
- [2] Chavarin JU 1991 *Corrosion* **47** (6) 472
- [3] Garverick L 1994 *Corrosion in petrochemical* (United States: ASM)
- [4] Ma L, Li W, Zeng H, Yan Y and Huo B 2010 *J. Chinese Soc. Corros. Prot.* **4** 2
- [5] Pratesa Y, Ferdian D and Togina I 2017 *IOP Conf. Ser. Mater. Sci. Eng.* **204** 12026
- [6] Wu D, Yan S, Wang, Zhang Z, Miao R, Zhang X and Chen D 2014 *J. Rare Earths* **32** 663
- [7] Sun M, Hu X, Peng L, Fu P and Peng Y 2015 *J Mat Sci Eng A* **20** 89
- [8] Yuansheng H Z R and Hong Y 2013 *J. Rare Earths* **31** 916
- [9] Salinas D R, Bessone J B, Garcia S G 1999 *J. Appl. Electrochem.* **29**
- [10] Lameche-Djeghaba S, Benchettara A, Kellou F 2013 *Arab. J. Sci. Eng.* **39** (1) 113
- [11] Raghavan V 2007 *J. Phase Equilibrium* **28** 556
- [12] Markoli B, Spaic S and Zupanic F 2001 *Z. Metallkd* **92** (9) 1098

Acknowledgement

The authors are grateful to PT Inalum for providing the aluminium ingot and Direktorat Riset dan Pengabdian Masyarakat (DRPM-UI) through PITTA 2017 grant for the financial support.